Strength analysis of capacitor energy storage cabinet of monorail elevated train

Guojing Ye*, *Jinsong* Zhou, and *Bingshao* Li

Institute of Rail Transit, Tongji University, Shanghai, China

Abstract. Based on the actual parameters of the capacitor energy storage cabinet on the top of the monorail train, built the cabinet's finite element model. Then, according to EN 12663-1, set the calibration conditions and fatigue working conditions. Carried out the simulation calculation under different conditions, respectively. The calculation results under the static calibration conditions show that the maximum equivalent stress of each node on the model is smaller than the allowable stress under all working conditions. Therefore, the static strength of the cabinet meets the design requirements. Plotted Goodman fatigue limit diagrams of the cabinet's base metal and weld and modified them in the Smith form. Then plotted the average stress and stress amplitude under fatigue working conditions in the corresponding scatter diagram. The diagram s show that all points are located within the permitted area. The results show that the fatigue strength of the cabinet meets the requirements of design and use.

Keywords: Capacitor cabinet, FEA analysis, Static strength, Fatigue strength.

1 Introduction

In recent years, with the rapid development of urban rail transit, the application of capacitors as an energy storage element in rail vehicles is increasing. Its advantages include small volume, large capacity, long life, high charge-discharge efficiency[1]. Therefore, it is of great significance to study the strength of capacitor energy storage cabinets for improving the running stability and safety of rail vehicles[2]. There is an interaction between the auxiliary equipment and the body of the rail vehicle, and the coupling vibration will greatly impact the operation of the vehicle. Therefore, the structure design of railway vehicle auxiliary equipment is an essential part of the overall design of the train[3]. Using Goodman fatigue limit diagram to design and check railway products can ensure the safety and lightweight of components under any cyclic load[4, 5], so Goodman fatigue limit diagram is widely used in the fatigue analysis of rail transit equipment. By using the Goodman fatigue limit diagram, H Wang[6] verified the fatigue strength of the welded frame of Y25 bogie. And J Cheng[7] calculated and analyzed the fatigue strength of a DC

* Corresponding author: yeguojing@tongji.edu.cn

converter under a metro vehicle. However, the research on the strength of auxiliary equipment of vehicles is mainly focused on the equipment under the vehicle. There are few researches on the strength of the auxiliary equipment on the top of the train.

In this paper, the capacitor energy storage cabinet on the roof of the monorail elevated train is taken as the research object, and its finite element model is built. The grid of the equipment's weld position is refined. Based on the finite element model, the static strength verification conditions are set according to the standard EN 12663-1[8], and the static strength verification analysis is carried out. Set fatigue strength conditions to calculate and analyze fatigue strength based on the Goodman fatigue limit diagram. This paper provides a reference for the subsequent strength calculation and analysis of rail vehicle auxiliary equipment.

2 Finite element model

The capacitor energy storage cabinet is installed on the top of the monorail and connected with the train body through elastic bases. The main structure of the cabinet is a frame structure. The maximum external dimension of the cabinet is 2494mm×1936mm×480mm. The total weight of the cabinet is 1090kg. The three-dimensional solid model of the energy storage cabinet is shown in figure 1.

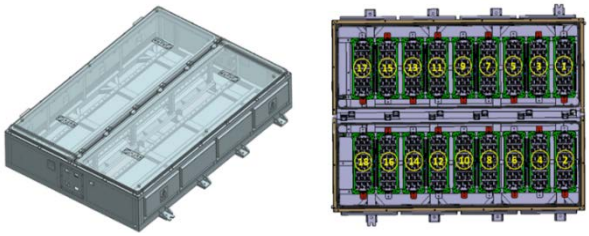

Fig. 1. 3D model of the energy storage cabinet.

The cabinet body and topside plate are welded with plates made by 6082-T6 aluminum alloy, the base is made of SUS304 stainless steel, and the rubber buffer between the base and the cabinet body is made of Thailand No.3 smoked sheet. The specific parameters of the metal material are shown in table 1.

Table 1. The material parameters of metal.

	Young's modulus (GPa)	Poisson's ratio	Density (kg/m^3)	Yield strength (MPa)	Tensile strength (MPa)
Base metal	72.5	0.33	2700	260	310
Weld	\	\	\	175	215
Base	210	0.3	7850	310	620

The specific parameters of the rubber material are shown in table 2.

Table 2. The material parameters of rubber.

	Shore hardness	Tensile strength (MPa)	Stiffness K_X:K_Y:K_Z (N/mm)
Rubber	65	>15	189:179:1227

When building the cabinet's finite element model, use two-dimensional elements to discretize the main structure of the model, and use three-dimensional elements to discretize the base part of the model. For the position where stress concentration may occur, especially the weld, carry out the element refinement treatment. The element size of the refined part is treated as 4mm. The energy storage units in the energy storage cabinet are simplified to quality points. For the main structure of the whole model of the cabinet, the

total number of elements is 468548, the number of nodes is 304344. For the weld part of the cabinet, the number of elements is 43881, the number of nodes is 57201. The finite element model of the energy storage cabinet is shown in figure 2 and figure 3.

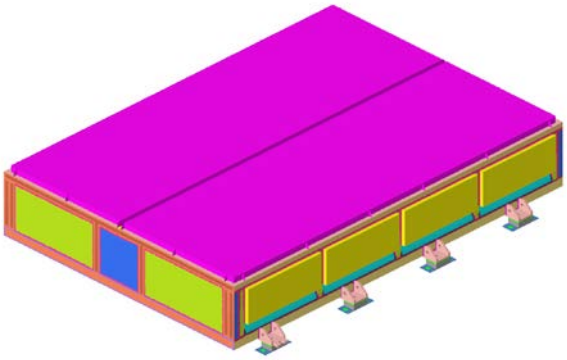

Fig. 2. Finite element model of the cabinet (with door).

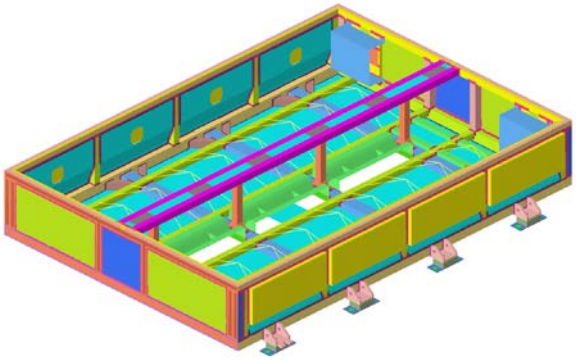

Fig. 3. Finite element model of the cabinet (without door).

3 Static strength analysis

3.1 Calibration conditions

According to the classification of passenger carriages in EN 12663-1[8], it is determined that the train belongs to category P-IV vehicle. According to load conditions table of car body's accessory equipment in the standard, the calibration acceleration is obtained as shown in table 3. Among them, the load corresponding to the condition 9 represents the load under the hoisting condition.

Table 3. Static strength calibration conditions.

Direction of loads	Condition Number								
	1	2	3	4	5	6	7	8	9
X	2g	2g	2g	2g	-2g	-2g	-2g	-2g	\
Y	1g	1g	-1g	-1g	1g	1g	-1g	-1g	\
Z	(1+*c*)g	(1-*c*)g	(1+*c*)g	(1-*c*)g	(1+*c*)g	(1-*c*)g	(1+*c*)g	(1-*c*)g	-1g

In the above table, *c* equals 2 for the rear position, and it changes linearly to 0.5 in the center of the vehicle. According to the actual situation of the assembly position of the energy storage cabinet, parameter *c* equals 2. And g is the acceleration of gravity, and its value is 9810 mm/s^2.

3.2 Calculation and analysis of static strength

Under the conditions of calibration, check the static strength of the cabinet according to the yield strength. The formula of allowed stress is as follow:

$$\sigma_c = R/S_1 \tag{1}$$

In the above formula, σ_c is allowed stress. S_1 is the safety factor of failure limit which equals 1.15 here. R is the ultimate strength of material. Substitute the specified value into the formula, then we can obtain the results. For 6082-T6 metal, the allowable stress σ_{c1} equals 226 MPa; for SUS304 metal, the allowable stress σ_{c2} equals 269 MPa.

After the simulation, the results of condition 9 and the stress analysis diagrams are obtained. The Von Mises equivalent stress and the detail diagram of the maximum stress position under condition 1 are shown in figure 4. The stress diagram of condition 2~8 is similar to that of condition 1, and the maximum stress appears around the bolt hole of the end base of the energy storage cabinet.

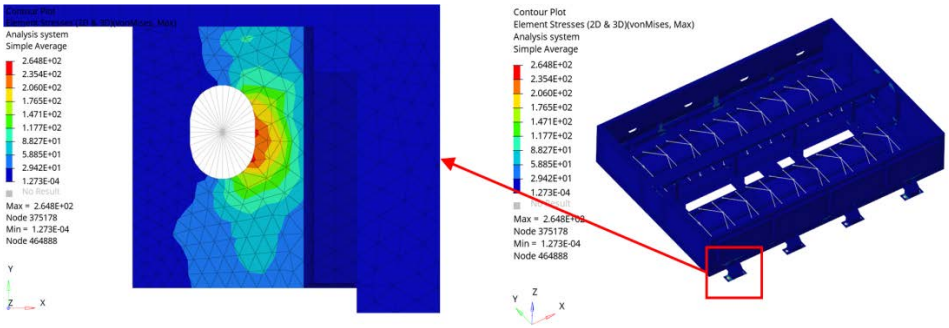

Fig. 4. Diagram of Von Mises stress under condition 1.

The equivalent stress diagram of condition 9 (the hoisting condition) is shown in figure 5. The results show that the position of maximum stress is around the hanging hole of the end base of the energy storage cabinet.

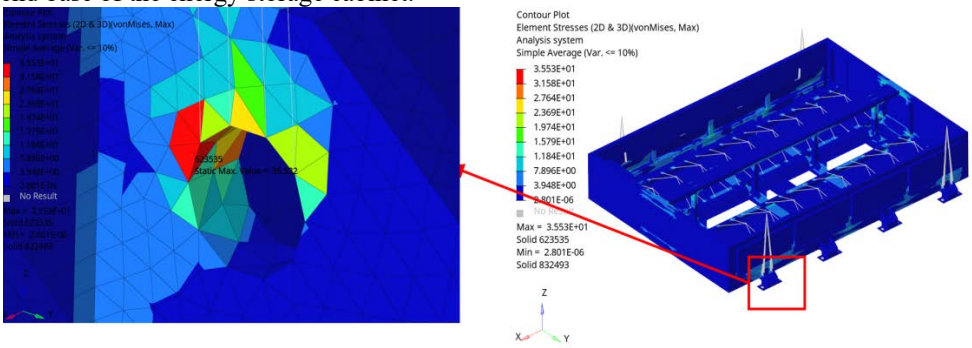

Fig. 5. Diagram of Von Mises stress under condition 9.

The statistics of the maximum equivalent stress of the energy storage cabinet under the static strength load are shown in table 4. The results show that the maximum equivalent stress under each working condition is less than the allowable stress, and the load factor is greater than the safety factor which equals 1.15. Therefore, the static strength of the energy storage cabinet meets the design requirements.

Table 4. Maximum stress under static strength load conditions.

Condition Number	1	2	3	4	5	6	7	8	9
Maximum stress(MPa)	264.8	109.5	228.4	131.8	264.4	106.2	230.9	138.3	35.53
Calibration coefficient	1.17	2.83	1.36	2.35	1.17	2.92	1.34	2.24	7.32

4 Fatigue strength analysis

4.1 Fatigue working conditions

According to the provisions of EN 12663-1 for fatigue load of monorail body's accessory equipment, the fatigue strength conditions are determined as shown in table 5.

Table 5. Fatigue strength working conditions.

Direction of loads	**Condition Number**							
	10	11	12	13	14	15	16	17
X	+0.2g	+0.2g	+0.2g	+0.2g	-0.2g	-0.2g	-0.2g	-0.2g
Y	+0.15g	+0.15g	-0.15g	-0.15g	+0.15g	+0.15g	-0.15g	-0.15g
Z	+1.15g	+0.85g	+1.15g	+0.85g	+1.15g	+0.85g	+1.15g	+0.85g

For the longitudinal direction, the equivalent fatigue load is the load caused by traction and braking. For the transverse and vertical direction, the equivalent fatigue load is the load caused by the vertical, transverse and torsional irregularity of the track. When using these equivalent loads, it is acceptable to take the material fatigue strength at 10^7 cycles as the allowable stress.

4.2 Calculation and analysis of fatigue strength

The calculation of the cabinet body is carried out to obtain the diagram of equivalent stress analysis. Under condition 10, the diagram of the equivalent stress and the larger image of the maximum value's position is shown in the figure. The diagrams of equivalent stress in working condition 11~17 are similar to that of condition 10. The maximum equivalent stress position under each condition is located at the connection between the lower longitudinal and lower cross beams.

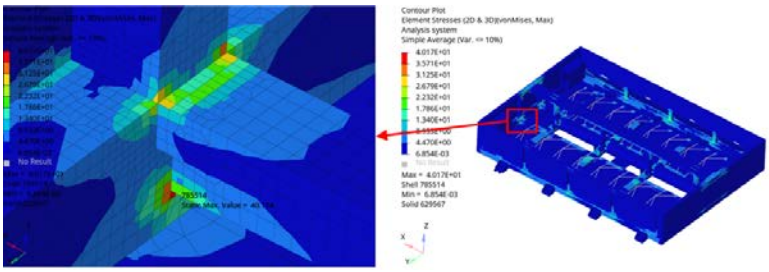

Fig. 5. Diagram of Von Mises stress under condition 10.

The maximum equivalent stress values of the cabinet under fatigue conditions are shown in table 6. The results show that the stress under fatigue conditions meets the design requirements.

Table 6. Maximum equivalent stress under fatigue working conditions.

Condition Number	10	11	12	13	14	15	16	17
Maximum stress(MPa)	40.17	29.3	39.69	28.81	43.71	32.84	43.23	32.25

Goodman fatigue limit diagram is used to analyse the fatigue strength calculation results under 10^7 load cycles[9, 10]. The yield strength and tensile strength of 6082-T6 base metal and weld of the cabinet are shown in Table 2.1. On this basis, the safety factor F is taken as 1.15 and used to check the fatigue strength[8]. The modified strength limit, yield limit, and fatigue limit of the 6082-T6 base metal are 269.6MPa, 226.1MPa, and 119.2MPa. The modified strength limit, yield limit, and fatigue limit of the 6082-T6 weld are 187.0MPa, 152.2MPa and 86.1MPa. Based on the above data, the modified Goodman fatigue limit diagram in the form of the Smith diagram is drawn, as shown in figure 6.

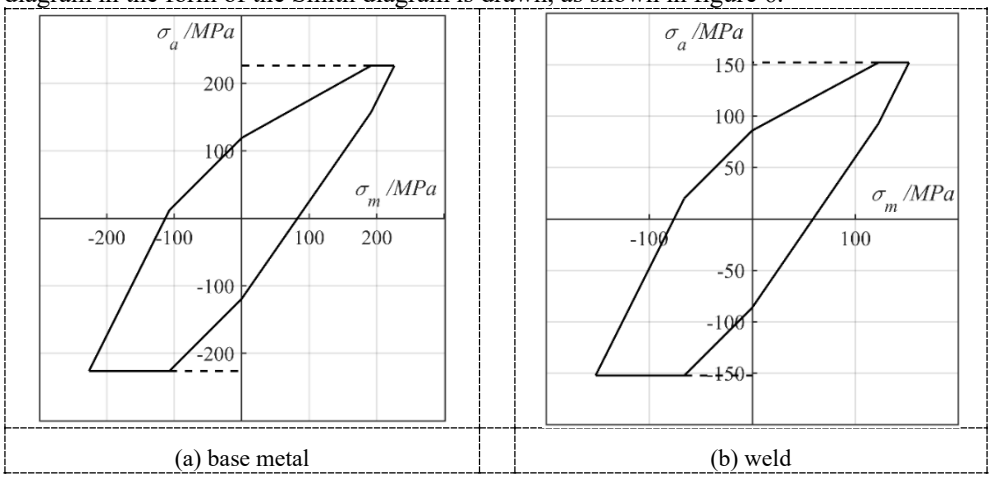

(a) base metal (b) weld

Fig. 6. Modified Goodman fatigue limit diagram in the form of Smith diagram.

In the fatigue assessment, the stress state of each node is simplified as a uniaxial stress state based on the maximum principal stress direction for conditions 10~17. The maximum and minimum stress values of each node are calculated. Calculate the average stress according to the following formula:

$$\sigma_m = (\sigma_{\max} - \sigma_{\min}) / 2 \tag{2}$$

where σ_m is the average stress; $\sigma_{\max}$ is the maximum stress; $\sigma_{\min}$ is the minimum stress. The calculation formula of stress amplitude is as follows:

$$\sigma_a = \sigma_{\max} - k\sigma_{\min} \tag{3}$$

where k is the conversion factor. For the base metal, take k as 0.7; For the weld, take k as 1. The obtained results are plotted in the Goodman fatigue limit diagram in scatter points, as shown in figure 7.

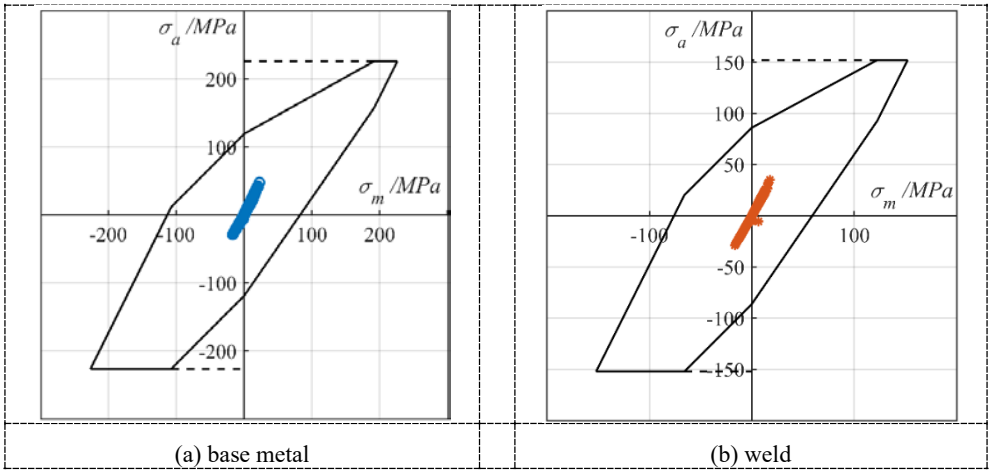

(a) base metal (b) weld

Figure 7. Modified Goodman fatigue limit diagram of calculated results.

It can be seen from the figure that for the base metal and weld of the cabinet, the stress points of each node are within the safe stress limit area, so the fatigue strength of the energy storage cabinet meets the use requirements. The number and location of the five nodes with the largest stress amplitude are shown in figure 8. The results show that the five nodes are located in the welding position of the upper longitudinal beam and the column in the cabinet.

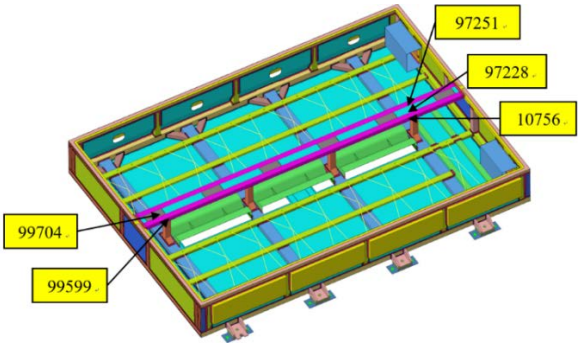

Fig. 8. Diagram of the position of the five nodes with the largest stress.

5 Conclusion

The use of sections to divide the text of the paper is optional and left as a decision for the author. Where the author wishes to divide the paper into sections the formatting shown in table 2 should be used.

(1) By the static strength analysis, the stress distribution of the cabinet is obtained. The results show that the Von Mises stress of the base metal and all joints of the welding seam are less than the allowable stress, and the static strength of the energy storage cabinet meets the design requirements.

(2) Under the static strength condition, the maximum stress position is the base connected with the car body at the end of the cabinet. Therefore, the base structure design can be improved further.

(3) Through fatigue strength analysis, Goodman fatigue limit diagrams of base metal and weld of the cabinet are obtained, respectively. The results show that the average stress

and stress amplitude combination points of the base metal and weld are within the limited area. Therefore, the fatigue strength of the cabinet body meets the relevant design requirements, and the safety margin is sufficient.

(4) The maximum stress amplitude position of the cabinet body appears at the weld between the upper longitudinal beam and the column in the cabinet body, so the structure can be strengthened further to optimize the fatigue strength of the energy storage cabinet.

References

1. Yang, J., Li, F. Y., Song, R. G., & Fang, Y. (2011). Review of the utilization of vehicular braking energy in urban railway transportation. Journal of the China railway society, 2(010).
2. DING, J., & RONG, Z. L. (2008). Structure Analysis of the Converter Cabinet Based on ProE-ANSYS [J]. Converter Technology & Electric Traction, 2.
3. Gong D. , Zhou J. , Du S. , Sun W. , & Sun Y. . (2016). Study on the effect of the underframe equipment on vibration transmissibility and modal frequency of the car body for high-speed emu trains. Journal of Mechanical Engineering, 52(18), 126-133.
4. Xiang, B., Shi, J., Guo, L., Liu, X., Liu, S., & Lin, J. (2002). Plotting and application of Goodman fatigue limit diagram of railway common materials. China Railway Science, 23(4), 72-76.
5. Huang, Y. M., & Wang, T. S. (1999). Two–axle bogie design for electrical multiple unit. Part 2: Bogie frame fatigue test. International Journal of Materials and Product Technology, 14(1), 102-122.
6. Wang, H., Liu, W. X., & Shang, Y. J. (2013). Fatigue strength analysis on welded frame of domestic Y25 bogie based on hot spot stress. China Railway Science, 34(4), 66-70.
7. CHENG, J., & ZHOU, J. The strength simulation of the subway trains.
8. Railway application - structure requirement of railway vehicle bodies: EN12663 -2010. Brussels: CoertoEuropeen de Normalisation , 2010.
9. Zhao, Y. X., Yang, B., Peng, J. C., & ZHANG, W. H. (2005). Drawing and Application of Goodman-Smith Diagram for the Design of Railway Vehicle Fatigue Reliability [J]. China railway science, 6.
10. Reihanian, M., Sherafatnia, K., & Sajjadnejad, M. (2011). Fatigue failure analysis of holding U-bolts of a cooling fan blade. Engineering Failure Analysis, 18(8), 2019-2027.